

Maximal power extraction strategy in the transition region and its benefit on the AEP (annul energy product)[†]

Yoonsu Nam¹, Jeong-gi Kim^{1,*} and Carlo L. Bottasso²

¹Department of Mechanical and Mechatronics Engineering, Kangwon National University, Hyoja 2-dong, Chunchon, Kangwon, 200-701, Korea

²Dipartimento di Ingegneria Aerospaziale, Politecnico di Milano, Via La Masa 34, Milano, 20156, Italy

(Manuscript Received November 17, 2010; Revised February 24, 2011; Accepted March 24, 2011)

Abstract

The rotational speed of a wind turbine is limited by the noise constraint of the blade tip speed. The larger the rotor diameter is, the smaller the rotor speed becomes. Therefore, there exists a transition region connecting the max-C_p operation with the power regulation operation. A conventional pitch schedule in this region involves using a fixed pitch. However, if the variable pitch instead of the fixed one is allowed, more electric power can be extracted from the wind. The benefit of using this strategy is analyzed from the point of how much the electric energy can be gained by applying the variable pitch schedule in this transition region.

Keywords: Wind turbine; Tip speed noise constraint; Variable speed variable pitch; Generator torque schedule; Annual energy product; Drive train model

1. Introduction

A wind turbine is an energy conversion machine that has to be designed to have the maximum efficiency in converting wind power to electric power. There are other design criteria for a wind turbine control system in addition to the machine efficiency. Because the wind turbine should operate for more than 20 years, the control system has to manage the mechanical loads of the machine structure such as the blades, the gearbox, and the tower below the certain level of magnitudes in order to prevent fatigue failures of the mechanical components of the machine. The other point is the noise constraint coming from the blade tips. It is known that the blade tip speed should be maintained below around 75 m/s to meet the noise level requirement of the on-shore wind turbine [1].

The modern control system for multi-MW wind turbines is designed based on the variable-speed and variable-pitch (VSVP) control concept [2-5]. Depending on the wind speed, the operational regimes of the wind turbine are divided into three regions. In the low wind speed region, the wind turbine is operated so as to extract the maximum energy from the wind. This region is called as the max-C_p region, where the rotor speed is varied with the wind speed by controlling the generator reaction torque. In this region, the blade pitch is fixed at a certain angle to hold the max-C_p operation. A wind

turbine is designed to produce the rated electric power for the wind speed region higher than the rated wind speed. The electric power of the machine is regulated to the rated in this wind speed region by the variable pitch control. In this wind speed region, called the power regulation region, the mitigation of the mechanical loads of the wind turbine is more important than the efficiency of the wind energy capture. The wind speed region between those two operational regions is the transition region, on which this paper is focusing.

The tip speed of the rotor should be maintained below around 75 m/s because of the blade tip noise. Therefore, there should be some upper bound in the rotor speed to meet this requirement. The pitch in this condition is usually fixed at the same pitch angle as the one used for the max-C_p operation. A fixed rotor speed and the fixed pitch control is the conventional control strategy in the transition region. The efficiency of the wind power capture can be increased if variable pitch control is applied instead of fixed pitch. This paper proposes a variable pitch schedule in the transition region which claims that more wind energy harvesting is possible. The usefulness of this control strategy is investigated by calculating and comparing the annual energy product (AEP) at different wind conditions with the AEP for the wind turbine using the conventional fixed pitch control.

2. Control strategy of wind turbine

The mechanical power of an air mass which has a flow rate of dm/dt with a constant speed of v is given by

[†]This paper was recommended for publication in revised form by Associate Editor Hyoun Jin Kim

*Corresponding author. Tel.: +82 33 253 0840, Fax.: +82 33 257 4190

E-mail address: jeonggi@kangwon.ac.kr

© KSME & Springer 2011

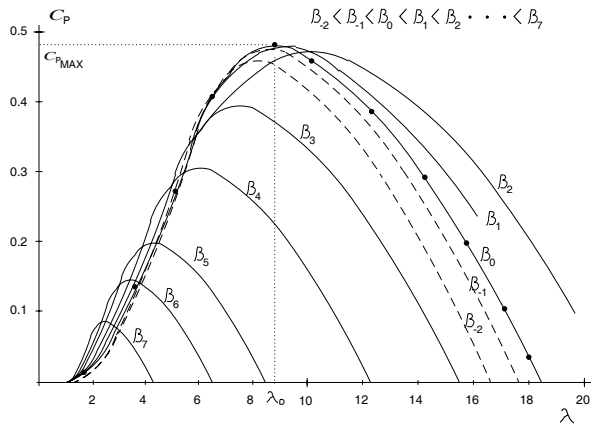


Fig. 1. Sample plot of C_p as a function of λ and β .

$$P_{wind} = \frac{d}{dt}(E) = \frac{d}{dt}\left(\frac{1}{2}mv^2\right) = \frac{1}{2} \frac{dm}{dt} v^2 = \frac{1}{2} \rho A v^3 \quad (1)$$

where ρ is the air density and A is the cross-sectional area of the air mass. Only a portion of the wind power given by Eq. (1) is converted to electric power by a wind turbine. The efficiency of the power conversion depends on the aerodynamic design and operational strategy of the wind turbine. Usually, the power generated by the wind turbine is represented by

$$P = C_p P_{wind} = C_p \left(\frac{1}{2} \rho \pi R^2 v^3\right) \quad (2)$$

where C_p represents the efficiency of wind power conversion and is called the power coefficient. R in the above equation is the rotor radius. The ideal maximum value of C_p is $16/27=0.593$, which is known as the Betz limit [6]. As shown in Fig. 1, the power coefficient, C_p is a function of pitch angle β and tip speed ratio λ which is defined as

$$\lambda = \frac{R\Omega_r}{v} \quad (3)$$

where Ω_r is the rotor speed of the wind turbine. The curve with dots shows the variation of C_p with λ for a fixed pitch angle of β_0 . As the pitch angle is away from β_0 , the value of C_p becomes smaller. Therefore, C_p has the maximum with the condition of $\lambda=\lambda_0$ and $\beta=\beta_0$. For a wind turbine to extract the maximum energy from the wind, the wind turbine should be operated with the max- C_p condition. That is, the wind turbine should be controlled to maintain the fixed tip speed ratio of $\lambda=\lambda_0$ with the fixed pitch of $\beta=\beta_0$ in spite of varying wind speed. Referring to Eq. (2), there ought to be a proportional relationship between the wind speed v and the rotor speed Ω_r to keep the tip speed ratio at constant value of λ_0 .

Fig. 2 represents a power curve which consists of three operational regions. Region I is max- C_p , Region II is a transition, and Region III is a power regulation region.

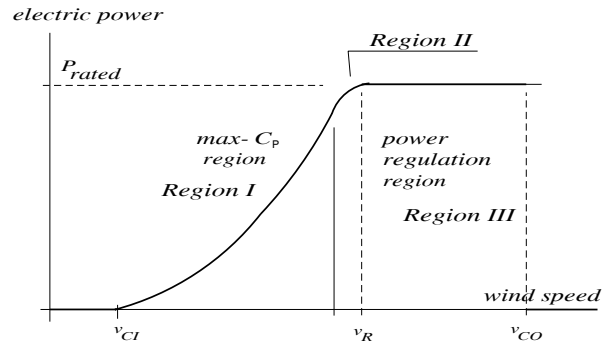


Fig. 2. Power curve.

- Region I: The wind turbine is operated in max- C_p . The blade pitch angle is fixed at β_0 and the rotor speed is varied so as to maintain the tip speed ratio constant (λ_0). Therefore, the rotor speed changes proportional to the wind speed by controlling the generator reaction torque. In the max- C_p region, only the generator torque control is active, while the blade pitch is fixed at β_0 .
- Region II: This is a transition region between the other two regions, that is, the max- C_p (Region I) and power regulation region (Region III). Several requirements, such as a smooth transition between the two regions, a blade-tip noise limit, minimal output power fluctuations, etc., are important issues in defining control strategies for this region.
- Region III: This is the above rated wind speed region, where wind turbine power is regulated at the rated power. Therefore, the rotor speed and the generator reaction torque are maintained at their rated values. In this region, the value of C_p has to be controlled so as to be inversely proportional to v^3 to regulate the output power to the rated value. This is easily checked by noting Eq. (2). In this power regulation region, the blade pitch control plays a major role.

3. Steady state analysis

3.1 Drive train model and torque scheduling of wind turbine

A wind turbine is a complicated mechanical structure which consists of rotating blades, shafts, gearbox, electric machine, i.e., generator, and tower. Sophisticated design codes are necessary for predicting a wind turbine's performance and structural responses in a turbulent wind field. However, the simple drive train model of Fig. 3 is sufficient for the control system design [7, 8]. The parameters referred to in Fig. 3 are summarized in Table 1. The aerodynamic torque developed by the rotor blades can be obtained using Eqs. (2) and (3) as follows:

$$\begin{aligned} T_a &= \frac{P}{\Omega_r} = \frac{1}{2} \rho \pi R^2 \frac{C_p(\lambda, \beta)}{\Omega_r} v^3 \\ &= \frac{1}{2} \rho \pi R^3 \left(\frac{C_p(\lambda, \beta)}{\lambda}\right) v^2 = \frac{1}{2} \rho \pi R^3 C_Q(\lambda, \beta) v^2 \end{aligned} \quad (4)$$

Table 1. Description of parameters in Fig. 3.

Symbol	Description	unit
J_r	Inertia of three blades, hub and low speed shaft	Kgm^2
J_g	Inertia of generator	Kgm^2
B_r	Damping of low speed shaft	Nm/s
B_g	Damping of high speed shaft	Nm/s
k_s	Torsional stiffness of drive train axis	N
c_s	Torsional damping of drive train axis	Nm/s
N	Gear ratio	-
T_g	Generator reaction torque	Nm
Ω_g	Generator speed	r/s

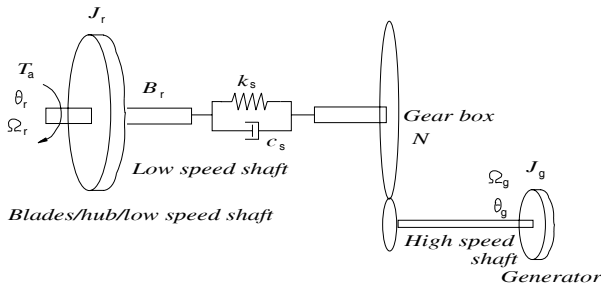


Fig. 3. Drive train model.

where $C_Q = C_p/\lambda$ is the torque coefficient. The aerodynamic torque of Eq. (4) is counteracted by the generator torque. Therefore, the governing equations of motion for a WT model of Fig. 3 are

$$\begin{aligned}
 J_r \frac{d\Omega_r}{dt} &= T_a - k_s(\theta_r - \frac{1}{N}\theta_g) - c_s(\Omega_r - \frac{1}{N}\Omega_g) - B_r\Omega_r \\
 J_g \frac{d\Omega_g}{dt} &= \frac{k_s}{N}(\theta_r - \frac{1}{N}\theta_g) + \frac{c_s}{N}(\Omega_r - \frac{1}{N}\Omega_g) - B_g\Omega_g - T_g
 \end{aligned} \tag{5}$$

Fig. 4 shows the relationship between rotor speed (Ω_r) and torque on a high speed shaft ($(T_a)_{HSS}$). Several mountain-shaped curves in this figure represent the aerodynamic torque on a high speed shaft for different wind speeds and rotor speeds at a fixed pitch β_o . These curves are easily calculated using Eq. (4) and power coefficient data similar to the one of Fig. 1 for any specific wind turbine. On this plot, the max-Cp operational condition is shown as a dashed line, which satisfies the quadratic relation:

$$\begin{aligned}
 (T_a)_{HSS} &= \frac{1}{2N} \rho \pi R^3 \left(\frac{C_{Pmax}}{\lambda_o} \right) v^2 = \frac{1}{2N} \rho \pi R^3 \left(\frac{C_{Pmax}}{\lambda_o} \right) \left(\frac{\Omega_r R}{\lambda_o} \right)^2 \\
 &= \frac{1}{2N} \rho \pi R^5 \frac{C_{Pmax}}{\lambda_o^3} (\Omega_r)^2 = k_{op} \Omega_r^2.
 \end{aligned} \tag{6}$$

In the below rated wind speed region, a wind turbine is to be operated with the max-Cp condition to extract maximum

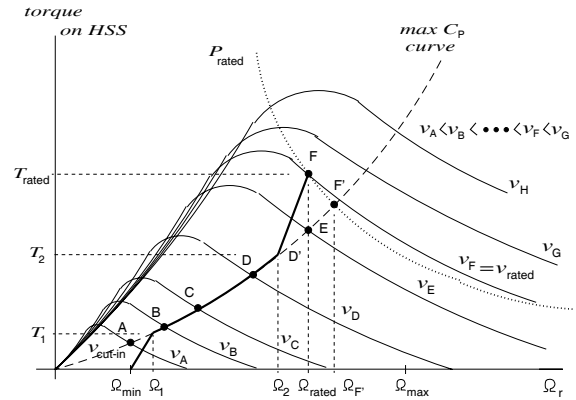


Fig. 4. Characteristic chart of torque on a high speed shaft and rotor speed.

energy from the wind. This means that the wind turbine should be operated at the point B for a steady wind speed v_B , the point C for a wind speed v_C , and so on in Fig. 4. For steady state operation, the aerodynamic torque of Eq. (6) should be counteracted by the generator reaction torque plus the mechanical losses from viscous friction, i.e., $B_r\Omega_r/N$ and $B_g\Omega_g$. Considering only the maximum energy capture, a generator torque schedule of A-B-C-D-E-F' is the optimal. However, the rated rotor speed might not be allowed to be as large as $\Omega_{F'}$ because of the noise problem. If the tip speed ($R\Omega_r$) of a rotor is over around 75 m/s, then noise from the rotor blades could be critical for on-shore operation. Therefore, as the size of a wind turbine becomes larger, the rated rotor speed becomes smaller. Because of this constraint, the torque schedule for most multi-MW wind turbines has the shape of either A-B-C-D-E-F or A-B-C-D'-F.

3.2 Steady state analysis

Not considering the noise constraint explained in the former section, the rotor speed at the rated power (P_{rated}) could be increased to the value

$$\Omega_r = \frac{\lambda_0}{R^{5/3}} \sqrt[3]{\frac{2P_{rated}}{\rho \pi C_{Pmax}}} \tag{7}$$

where λ_0 and C_{Pmax} represent the tip speed ratio and the power coefficient at the max-Cp condition. Fig. 5 shows the steady state operational status of a wind turbine for each wind speed. The solid lines marked with '◇' in this figure represent the steady state conditions when the noise constraint is applied while the dashed ones marked with 'x' are those when that is not. The first plot in this figure shows the relation of the rotor speed with the wind speed. The wind turbine would reach the rated operation with the rotor speed of 18.98 rpm and the wind speed of 11.2 m/s, if there was no noise constraint. However, the rated rotor speed should be decreased to 15 rpm and the rated wind speed would be 12.3 m/s, if considering the noise constraint. The vertical lines in this figure are used to identify

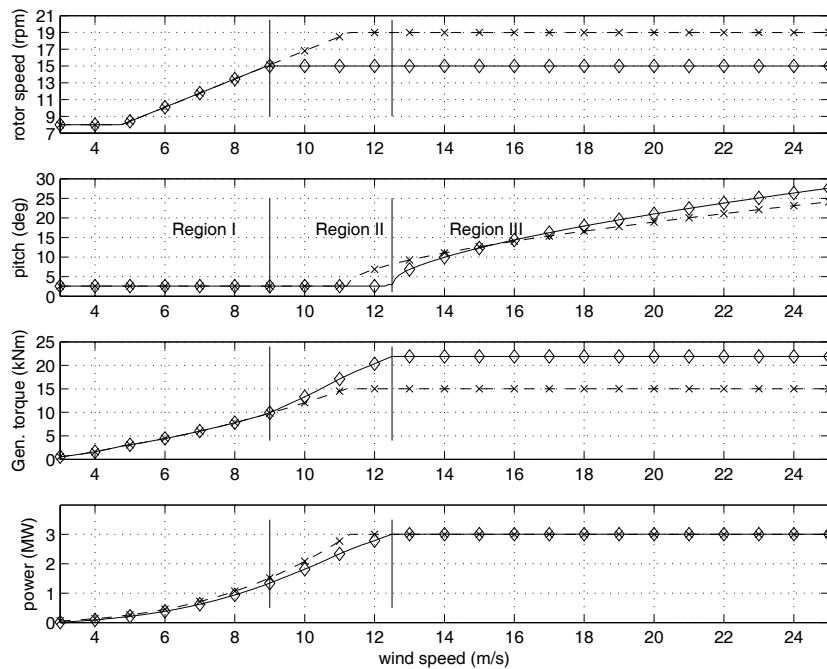


Fig. 5. Steady state characteristic chart of the rotor speed, pitch, generator torque, and power for a multi-MW wind turbine. The solid lines marked with ‘◇’ represent the steady state conditions when the noise constraint is applied while the dashed ones marked with ‘x’ are those when that is not.

the operational regions for the wind turbine, which is designed with the noise constraint. The second one shows the pitch schedule for the wind speed. The third and fourth one are the generator torque and the electric power in the steady state. These data are drawn from a 3 MW wind turbine. As shown in the final plot, much more electric power can be extracted from the wind if there is no constraint of the tip speed noise.

The steady state characteristics of Fig. 5 can be calculated using Eq. (5). For the steady state operating condition, these two equations can be combined and become

$$\begin{aligned} & \frac{T_a}{N} - \frac{B_r \Omega_r}{N} - B_g \Omega_g - T_g \\ & = \frac{1}{2N} \rho \pi R^3 C_Q(\lambda, \beta) v^2 - \frac{B_r \Omega_r}{N} - N B_g \Omega_g - T_g = 0 \end{aligned} \quad (8)$$

Assuming that the scheduling of the generator torque, i.e., T_g in the above equation, is made as shown in Fig. 4 (i.e., A-B-C-D-E-F), two variables, the rotor speed and the pitch, are the only unknowns in the above algebraic equation for a given wind speed. As explained in Section 2, either the pitch or the rotor speed is fixed depending on the wind speed. Therefore, for a certain wind speed, only one variable is the unknown, and this can be determined by solving the nonlinear algebraic equation of Eq. (8).

3.3 Maximal power extraction in a transition region with the tip speed noise constraint

Assuming that the wind blows gently (without any turbulence) from the cut-in to the cut-out speed in a very gradual

change rate, the operational status of the wind turbine varies in a gentle way too. Fig. 6 shows how the wind turbine behaves on a C_p - λ chart for the above wind condition. The curve marked with dot represents the locus of the operational status of the wind turbine when it is operated with the tip noise constraint. The other curve marked with ‘+’ is the locus for the case of not considering this constraint.

First, refer to the solid lines marked with ‘◇’ in Fig. 5, which represent variations of the operational status for the wind turbine considering the tip noise constraint. Every point of the solid lines line marked with ‘◇’ in Fig. 5 is equivalent to the locus marked with dots on the C_p - λ chart of Fig. 6. For a gradual wind speed change from 3 m/s to 5 m/s, the C_p - λ locus starts from the rightmost point ($\lambda = 13$) and goes toward the C_p -max point at $\lambda = 8.2$ along the constant pitch curve of 2.6 degree. For the wind speed increase up to 9 m/s (the end of Region I), the wind turbine stays on the C_p -max point for a while. If the wind speed continuously increases to the rated of 12.3 m/s from 9 m/s, the wind turbine cannot hold the C_p -max operation and moves to the left side of the mountain-like C_p - λ chart along the same constant pitch line. The C_p descent ends at $\lambda = 6$. This is the steady behavior of the wind turbine in the Region II, which is also called the transition region. For a further increase of the wind speed to the cut-out, the wind turbine operational state moves down on the C_p - λ chart in order to regulate the electric power with the rated. In this region (Region III), the C_p and λ should have the relation of

$$C_p = C_{P_{MAX}} \left(\frac{\lambda}{\lambda_0} \right)^3. \quad (9)$$

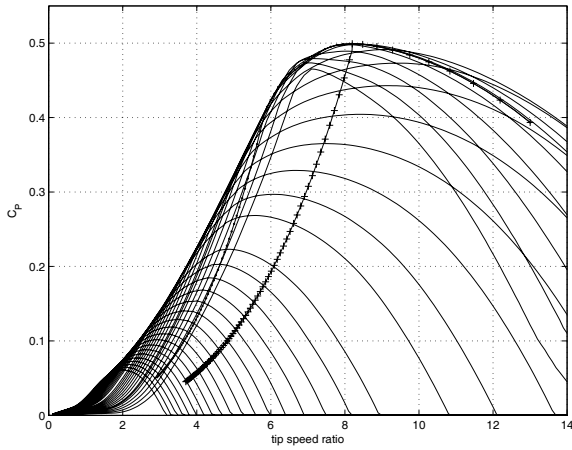


Fig. 6. Loci of steady state operation on a Cp-λ chart.

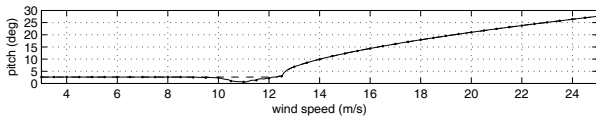


Fig. 7. Steady state pitch schedule which maximizes the energy extraction from the wind in the transition region (i.e. Region II) for a multi-MW wind turbine.

The above relation can be easily drawn from Eqs. (2) and (3) with the output power constraint of $P = P_{rated}$.

In case of not considering the noise constraint, the wind turbine has only two operation regions: the max-Cp region (Region I) and the power regulation region (Region III). Therefore, the wind turbine steady state operation, i.e., the Cp-λ locus marked with '+' in Fig. 6, does not have transition behavior. The Cp-λ locus drops from the Cp-max condition to the lower Cp point along the curve satisfying Eq. (9).

Closely examining the Cp-λ locus marked with dots of Fig. 6 in the transition region (i.e., λ in the range of 6~8.2), the locus is not located on the maximum-Cp envelope, which means that the wind turbine is not optimally operated in the sense of the maximal energy extracting strategy from the wind in the transition region. If the variable pitch instead of the fixed pitch of 2.6 degrees was applied in this region, the steady state operational status of the wind turbine would be on the maximum-Cp envelope. The variable pitch schedule in the transition region can be sought by solving an optimization problem with the constraint of Eq. (8) and maximum energy extraction. Fig. 7 shows this optimal variable pitch schedule. Note how the pitch varies in the transition region (i.e., wind speed from 9 m/s to 12.3 m/s) to extract the maximum energy from the wind.

4. AEP comparison

The benefit of the variable pitch schedule in the transition region over the conventional method, i.e., the method using a fixed pitch schedule, is verified through the AEP (annual energy product) comparison. The AEP is defined as the total

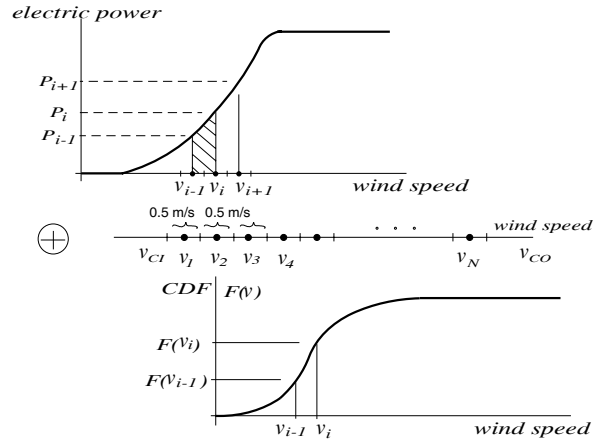


Fig. 8. Schematic diagram of AEP calculation.

wind energy captured by a wind turbine during a year, which can be represented as

$$AEP = \int_{1\text{ year}} P(t) dt = \frac{\pi R^2}{2} \int_{1\text{ year}} C_p \rho v^3(t) dt \quad (10)$$

In the calculation of AEP, the above relation is not appropriate, because it is virtually impossible to analytically express $P(t)$ or $C_p \rho v^3(t)$ as a function of t . Therefore, the AEP can be estimated only through a statistical way. Fig. 8 is the schematic diagram explaining the method of calculating AEP. The first step of this method is discretizing the wind speed. The full span of the wind speed from 3 m/s to 25 m/s is discretized into many wind speed bins having the width of 0.5 m/s. Then, the AEP can be determined by summing all contributions of each wind speed bin (i.e., like the hatched wind speed bin of Fig. 8). It is approximately given as [9]

$$AEP = \sum_{i=1}^N AEP_i = \sum_{i=1}^N \frac{(P_i + P_{i-1})}{2} \{F(v_i) - F(v_{i-1})\} \times 8760(\text{kwh})_i \quad (11)$$

where AEP_i = AEP produced by the i-th wind speed bin
 P_i = electric power for the wind speed of v_i
 $F(v_i)$ = cumulative probability distribution function (CDF).

The CDF, $F(v_i)$ can be obtained by integrating the Rayleigh probability distribution function and is given as

$$F(v_i) = \int_0^{v_i} \left\{ \frac{\pi}{2} \frac{v}{\bar{v}^2} e^{-\frac{\pi}{4} \left(\frac{v}{\bar{v}}\right)^2} \right\} dv = 1 - e^{-\frac{\pi}{4} \left(\frac{v_i}{\bar{v}}\right)^2} \quad (12)$$

where \bar{v} = mean wind speed.

The AEP results calculated based on Eq. (11) are summarized in Table 2. To evaluate the benefit of the proposed method, AEPs at eight different wind mean speeds (4, 5, 6, 7,

Table 2. AEP data for different WT operational strategies.

\bar{v} (m/s)	AEP (MWh)			$\frac{AEP_2 - AEP_1}{AEP_1} (\%)$	$\frac{AEP_3 - AEP_1}{AEP_1} (\%)$
	Fixed pitch (AEP1)	Variable pitch (AEP2)	No constraint (AEP3)		
4	1812.2	1813.4	2172.8	0.07	19.90
5	3560.6	3566.2	4128.6	0.17	15.97
6	5727.9	5741.4	6490.9	0.23	13.32
7	8029.2	8048.9	8918.7	0.25	11.08
8	10229.9	10253.6	11172.6	0.23	9.22
9	12183.0	12208.6	13124.3	0.21	7.73
10	13803.5	13829.5	14709.8	0.19	6.57
11	15051.4	15076.7	15904.8	0.17	5.67

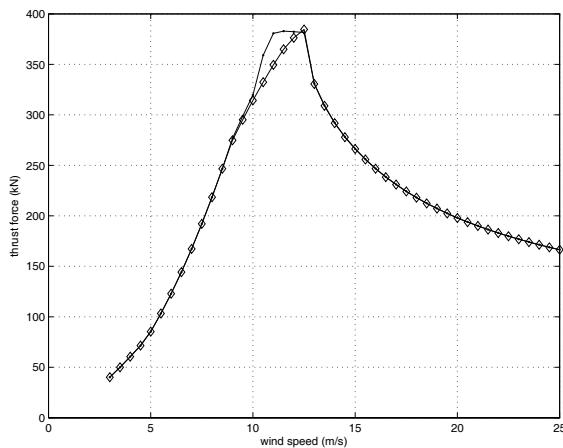


Fig. 9. Steady state thrust force variation with wind speed. The plot marked with ‘◇’ is the variation of the thrust force in case of using the fixed pitch, while the one with dot is for using variable pitch in the transition region.

8, 9, 10 and 11 m/s) are compared as shown in Table 2. The second column (denoted as AEP1) is the AEP which will be produced when the fixed pitch is used in a transition region. The third column (denoted as AEP2) shows the AEP in case of using the variable pitch schedule of Fig. 7. Finally, the fourth column (denoted as AEP3) has the AEP data when the wind turbine is operated without the consideration of the tip speed noise constraint. Approximately, the strategy of using the variable pitch (AEP2) in a transition region produces 0.2% more of AEP compared to that of using the fixed pitch (AEP1). Even though the amount of the AEP increase for the 3MW machine is not so great, the strategy of the variable pitch should be continuously investigated for a larger wind turbine.

If a wind turbine can be operated without the noise constraint, the increase of AEP would be huge as shown in Table 2. Therefore, the rotor blade design which minimizes the blade tip noise problem should be also considered in addition to the method of the variable pitch scheduling in the transition region.

One point which should be considered in selecting the pitch schedule in the transition region is the effect of this on the mechanical loads on the wind turbine structure. Fig. 9 shows

the steady state thrust force variation with the wind speed. In this figure, the plot marked with ‘◇’ is the variation of the thrust force in case of using the fixed pitch, while the one with dots is for using variable pitch in the transition region. As shown in this figure, the variable pitch schedule in the transition region produces more static thrust force than that for the fixed pitch schedule for the same wind speed. Although the variable pitch can extract more energy from the wind in transition region, it produces more static thrust force on blades, which might not be acceptable in the safety requirement of the wind turbine structural design.

5. Conclusions

There exists a transition region in which the max-Cp operation of the wind turbine is no more possible. The conventional pitch schedule in this region involves using a fixed pitch. It turns out this pitch schedule is not optimal from the point of the maximal energy capture from the wind. A variable pitch schedule which can extract more energy in the transition region than the fixed pitch schedule is proposed. The benefit of using the variable pitch schedule in a transition region is investigated. About 0.2% increase in the AEP is anticipated when applying the variable pitch schedule instead of the fixed pitch in the transition region.

Acknowledgment

This work was supported by a grant from the New & Renewable Energy division of the Korea Institute of Energy Technology Evaluation and Planning (KETEP) funded by the Ministry of Knowledge Economy, Republic of Korea (Grant No. 20103010020040 Grant name - Development of Control algorithm and system for Wind Turbine).

Nomenclature

- A : Area swept by the rotor
- B_r : Damping coefficient of the low speed shaft
- B_g : Damping coefficient of the high speed shaft
- C_p : Power coefficient

C_{PMAX}	: Maximum power coefficient
C_Q	: Torque coefficient ($=C_p/\lambda$)
c_s	: Torsional damping coefficient of the drive train axis
$F(v_i)$: Cumulative probability distribution function
J_r	: Inertia of 3 blades, hub, and low speed shaft
J_g	: Inertia of generator
k_s	: Torsional stiffness of the drive train axis
N	: Gear ratio
P	: Wind turbine electric power
R	: Rotor diameter
T_a	: Aerodynamic torque
T_g	: Generator reaction torque
v, v_i	: Wind speed
\bar{v}	: Mean wind speed
R	: Rotor diameter
β	: Pitch of the blade
λ	: Tip speed ratio
ρ	: Air density
Ω_r	: Rotor rotational speed
Ω_g	: Generator rotational speed

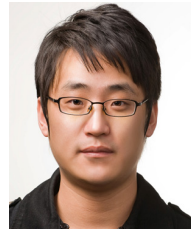
References

- [1] G. Leloudas, W. Zhu, J. Sorensen, W. Shen and S. Hjort, Prediction and reduction of noise for a 2.3MW wind turbine, *Journal of Physics: Conference series*, 75 (2007) 1-9.
- [2] T. Petru and T. Thiringer, Modeling of wind turbines for power system studies, *IEEE Trans. on Power Systems*, 17 (4) (2002).
- [3] F. D. Bianchi, H. D. Battista and R. J. Mantz, *Wind turbine control systems, principles, modeling and gain scheduling design*, Springer (2007).
- [4] E. A. Bossanyi, The design of closed loop controller for wind turbines, *Wind Energy*, 3 (2000) 149-163.
- [5] M. H. Hansen, A. Hansen, T. J. Larsen, S. Øye, P. Sørensen and P. Fuglsang, *Control design for a pitch-regulated, variable speed wind turbine*, Risø-R-1500(EN), (2005).
- [6] J. Manwell, J. McGowan and A. Rogers, *Wind energy explained, Theory, design and application*, A John Wiley and Sons (2009).
- [7] E. van der Hooft, P. Schaak and T. van Engelen, *Wind turbine control algorithm*, ECN-C-03-11 (2003).
- [8] W. Leithead and B. Connor, Control of variable speed wind turbines: dynamic models, *International Journal of Control*, 73 (13) (2000) 1173-1188.
- [9] IEC 61400-121, *Power performance measurements of grid*

connected wind turbines, International Electrotechnical Commission (2003).



Yoonsu Nam received the B.S. degree in nuclear engineering and M.S. degree in mechanical engineering from Seoul National University, Korea, in 1981 and 1983, and Ph.D. degree in mechanical engineering from Georgia Institute of Technology, Atlanta, in 1991, where he worked on the tip position control of a flexible manipulator using a proof mass. From 1992 to 1996, he was with the flight dynamics and control laboratory of the Agency for Defense Development in Korea. He is currently professor of mechanical and mechatronics engineering department, Kangwon National University in Korea. His main interest is the wind turbine control system design.



Jeong-gi Kim received the B.S. and M.S. degree in Mechanical and Mechatronics Engineering from Kangwon National University, Chuncheon, Korea, in 2009, and 2011, respectively. He is currently working for Control & Monitoring laboratory in Kangwon National University. His research interests are in

wind turbine control system design, load calculation and evaluation of wind turbine systems.



Carlo L. Bottasso received the Ph.D. degree in Aerospace Engineering from the Politecnico di Milano, Milan, Italy, in 1993. Currently, he is a Professor of Flight Mechanics with the Department of Aerospace Engineering, Politecnico di Milano, where he leads the POLI-Wind and POLI-Rotorcraft research

laboratories. He has held visiting positions at various institutions, including Rensselaer Polytechnic Institute, Georgia Institute of Technology, Lawrence Livermore National Laboratory, NASA Langley, and NREL among others. His research interests and areas of expertise include the flight mechanics and aeroelasticity of rotorcraft vehicles, aeroelasticity and active control of wind turbines, and flexible multibody dynamics.